Supporting Information

Efficient electrocatalytic conversion of CO_2 to syngas for Fischer-Tropsch process by partially reduced Cu_3P nanowire

Bing Chang[a], Xia-Guang Zhang[b], Zhaojun Min[b], Weiwei Lu[c], Zhiyong Li[b], Jikuan Qiu[b], Huiyong Wang[b], Jing Fan[a*], and Jianji Wang[b*]

[a] School of Environment, Key Laboratory for Yellow River and Huai River Water Environment and Pollution Control, Ministry of Education, Henan Normal University, Xinxiang, Henan, 453007, People's Republic of China

[b] School of Chemistry and Chemical Engineering, Key Laboratory of Green Chemical Media and Reactions, Ministry of Education, Henan Normal University, Xinxiang, Henan, 453007, People's Republic of China

[c] School of Chemical Engineering and Pharmaceutics, Henan University of Science and Technology, Luoyang, Henan, 471023, People's Republic of China

[*] Corresponding authors

E-mail address: fanjing@htu.edu.cn (Prof. J. Fan) and jwang@htu.edu.cn (Prof. J. Wang)

Table of Contents

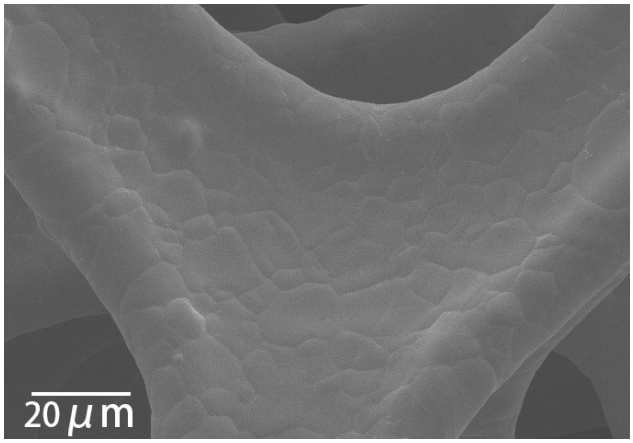

Fig. S1. SEM image of the bare copper foam.

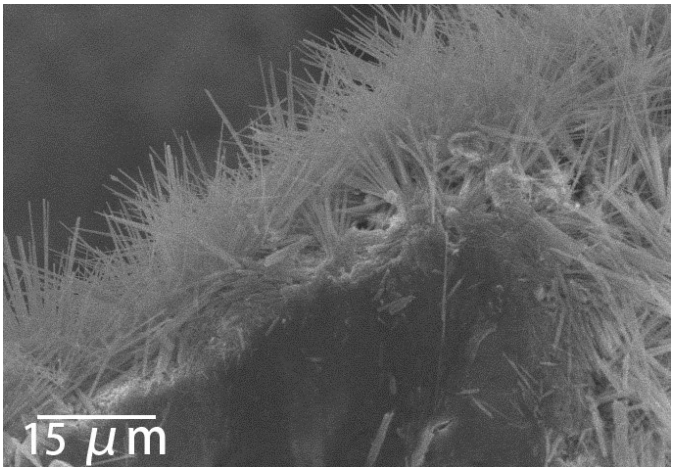

Fig. S2. Cross-section SEM image of the R-Cu_3P/Cu.

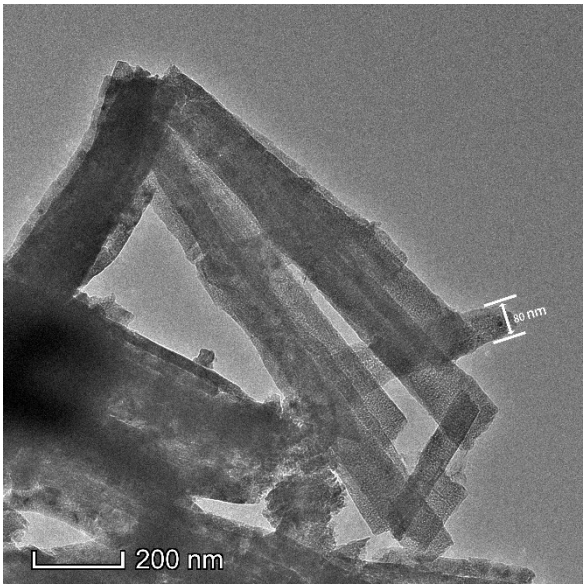

Fig. S3. TEM image of the R-Cu_3P/Cu.

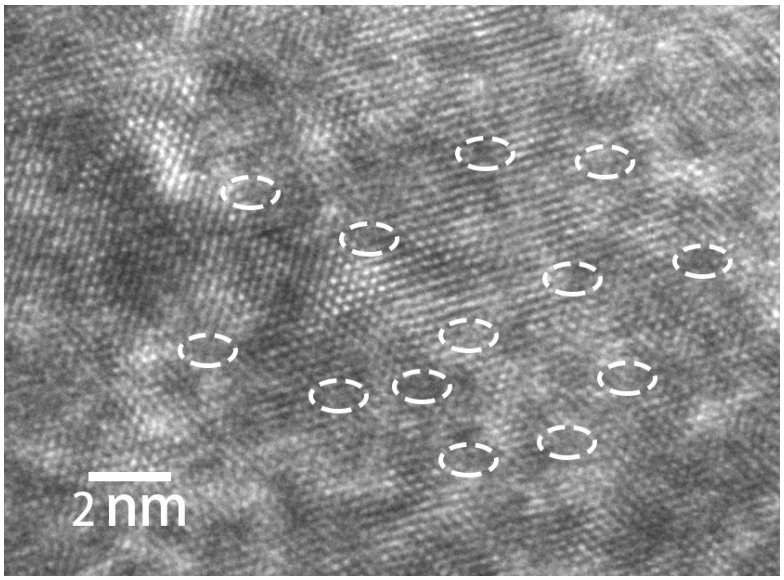

Fig. S4. HR-TEM partial enlarged image of R-Cu_3P/Cu.

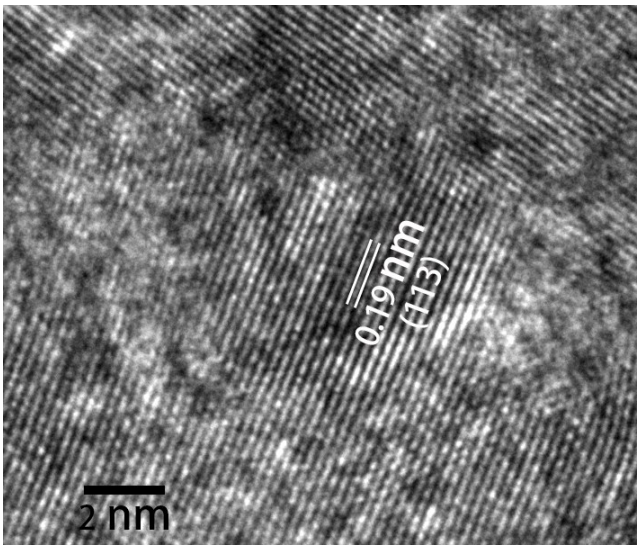

Fig. S5. HR-TEM image of the Cu_3P/Cu.

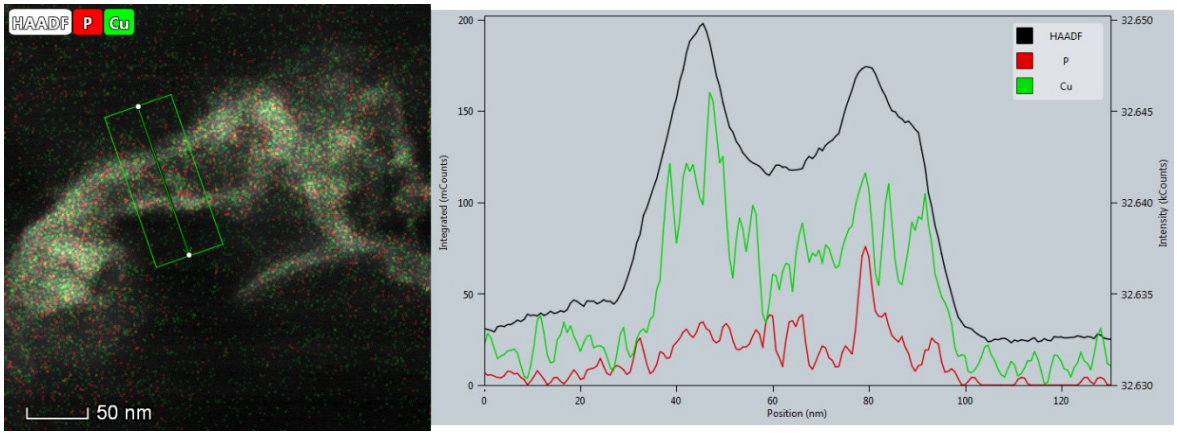

Fig. S6. HAADF image and corresponding EDS line scanning spectrum of R-Cu_3P/Cu.

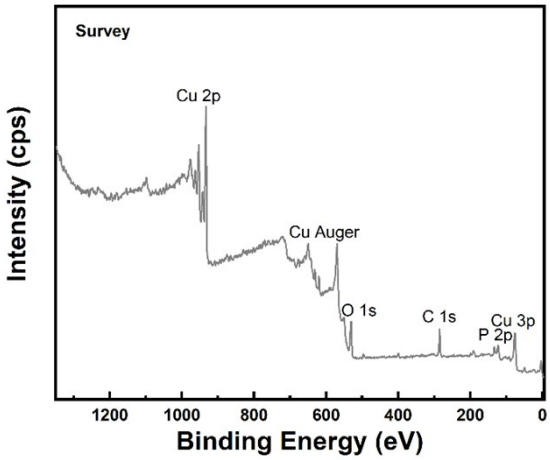

Fig. S7. XPS survey spectrum of R-Cu_3P/Cu.

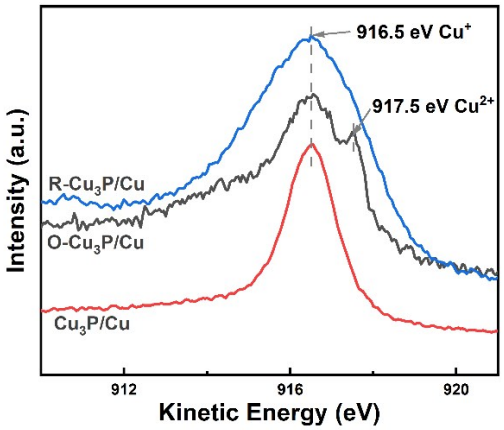

Fig. S8. AES spectra of Cu_3P/Cu, O-Cu_3P/Cu, and R-Cu_3P/Cu.

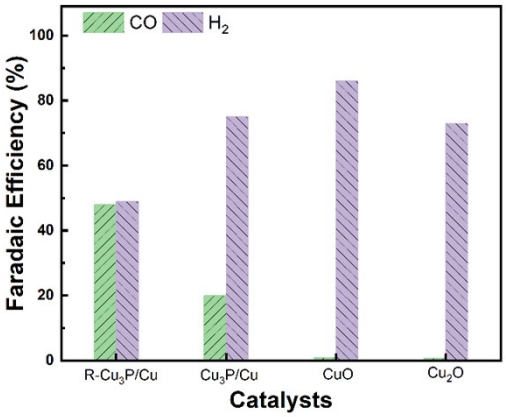

Fig. S9. CO and H_2 FE of R-Cu_3P/Cu, Cu_3P/Cu, CuO, and Cu_2O at -0.625 V *vs*. RHE.

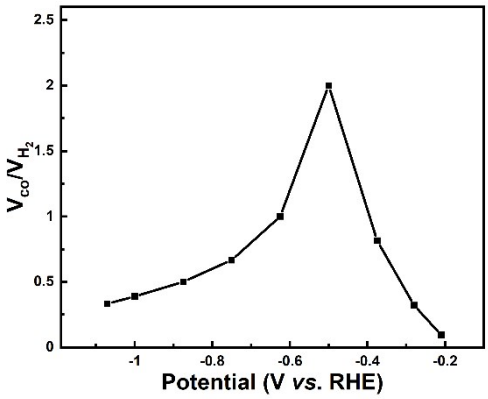

Fig. S10. The ratio of V_{co}/V_{H2} at different applied potentials.

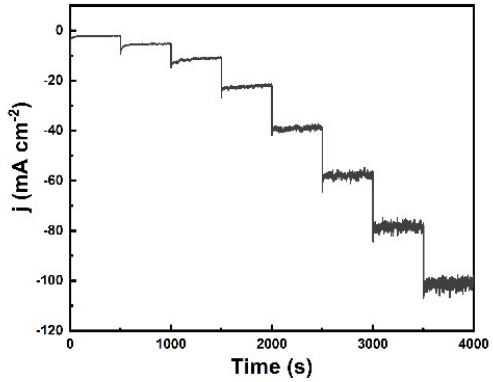

Fig. S11. Multi-potential process of R-Cu_3P/Cu in CO_2RR process. Each applied potential last for 500 s.

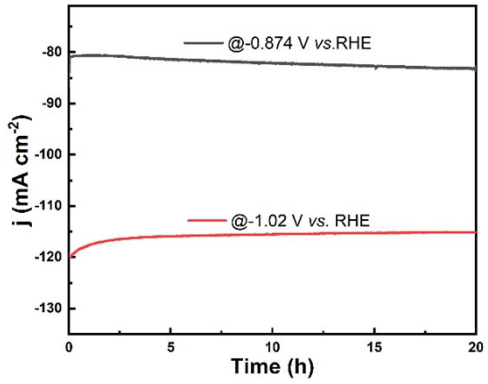

Fig. S12. Time-dependent current plots of R-Cu_3P/Cu in CO_2-saturated 0.5 M $NaHCO_3$ solution at preset potentials of -0.874 V (CO/H_2: 1/2) and -1.02 V (CO/H_2: 2/5).

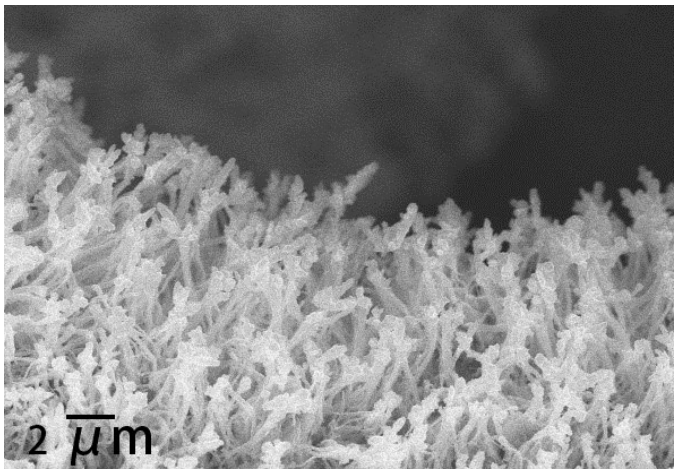

Fig. S13. SEM image of R-Cu_3P/Cu after 20 h potentiostatic electrolysis.

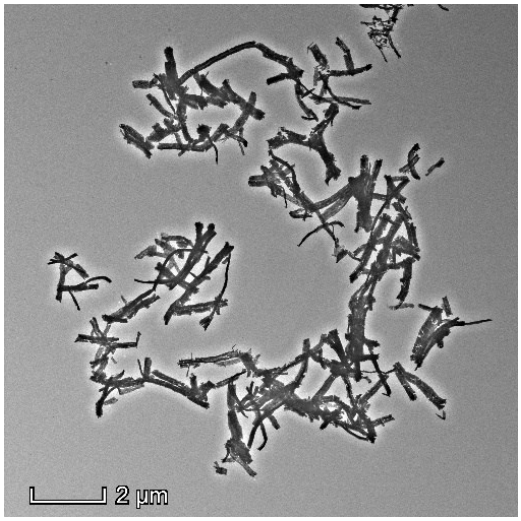

Fig. S14. TEM image of R-Cu_3P/Cu after long-term electrolysis.

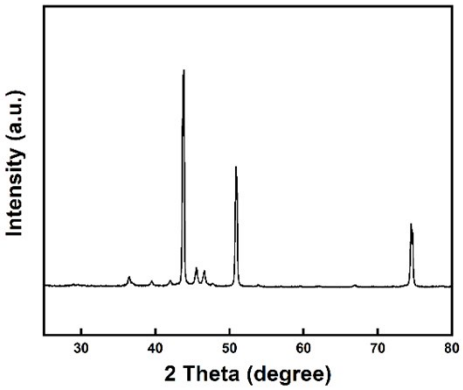

Fig. S15. XRD pattern of R-Cu_3P/Cu after long-term electrolysis.

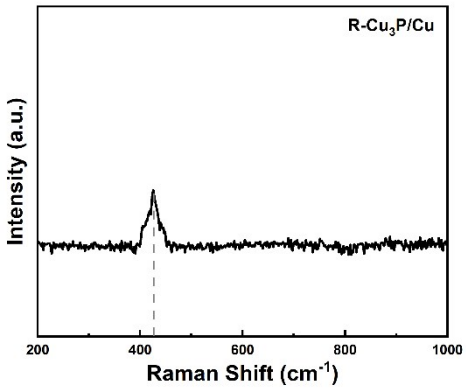

Fig. S16. Raman spectrum of R-Cu_3P/Cu after long-term electrolysis.

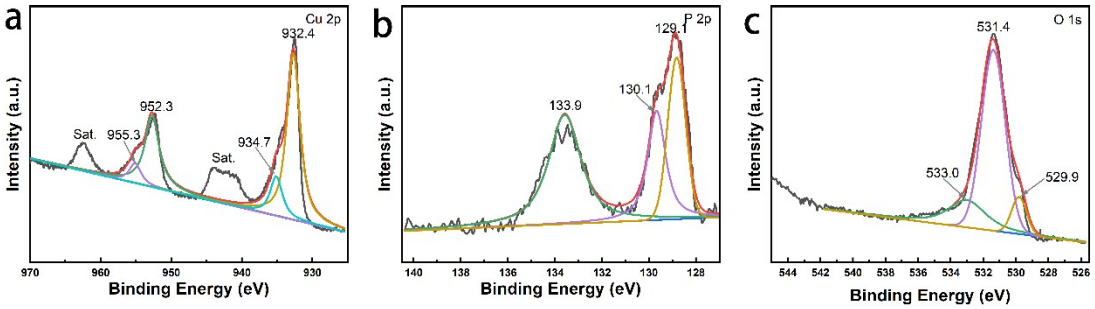

Fig. S17. High-resolution XPS spectra of R-Cu_3P/Cu after long-term electrolysis.

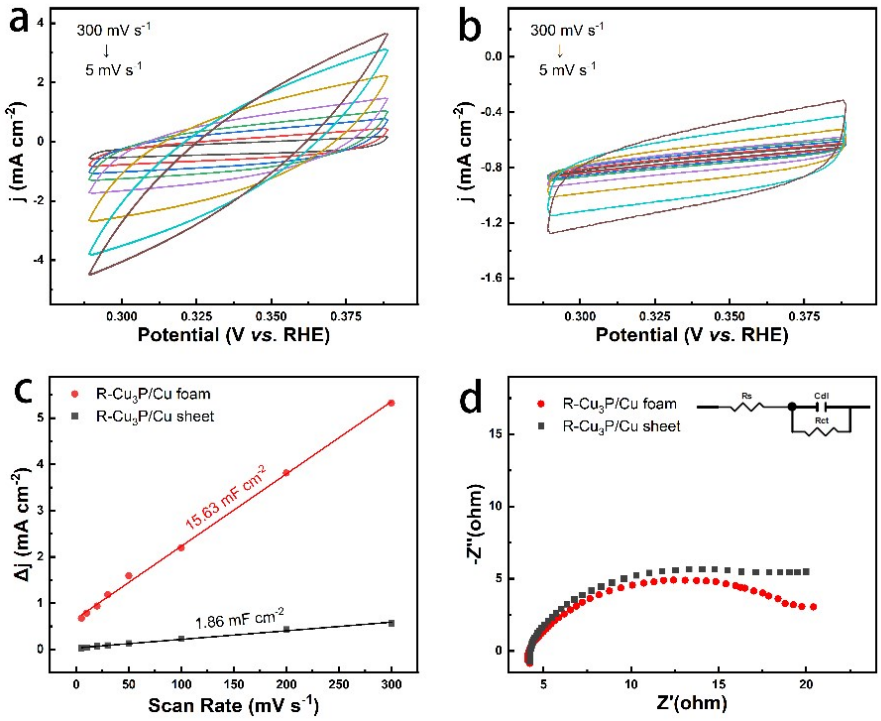

Fig. S18. CV curves of R-Cu_3P/Cu foam (a) and sheet (b) at different scan rates: 5, 10, 20, 30, 50, 100, 200, and 300 mV s^{-1} from inside to outside. (c) Capacitive current at 0.339 V (vs. RHE) as a function of the scan rate for R-Cu_3P/Cu foam and sheet ($\Delta j = j_a - j_c$). (d) Nyquist plots of R-Cu_3P/Cu foam and sheet in the frequency range of 0.1-100 KHz. Inset: Randles' equivalent circuit used for fitting the experimental impedance data. Note: solution resistance (R_s), electrical double-layer capacitance (C_{dl}), charge transfer resistance (R_{ct}).

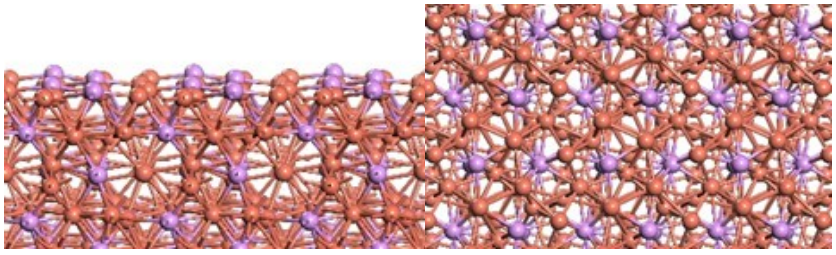

Fig. S19. Side and vertical view of the optimized structures of Cu_3P.

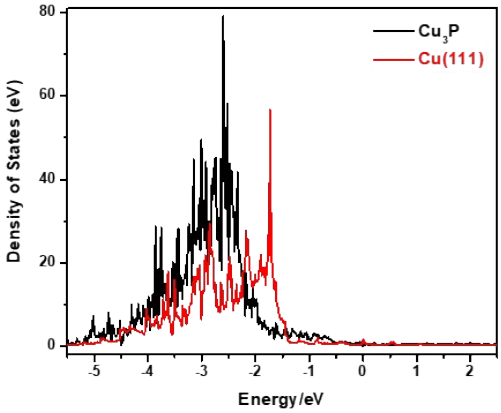

Fig. S20. DOS of *d*-electrons for the surface Cu atoms of Cu_3P and Cu (111) surface. The energy is relative to the Fermi level.

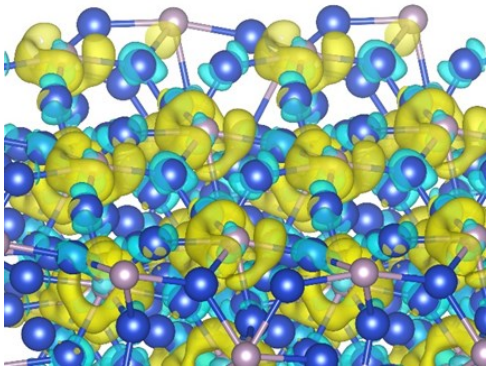

Fig. S21. Charge density difference of Cu and P on the bulk Cu_3P as defined by: $\Delta\rho = \rho_{Cu3P} - \rho_{Cu} - \rho_{P}$. The yellow and green area represents electron accumulation and depletion, respectively.

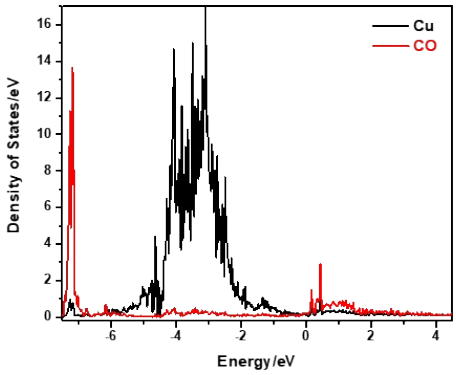

Fig. S22. DOS of *d*-electrons for the surface Cu atoms of Cu_3P and *s*, *p*-electrons for the adsorbed CO. The energy is relative to the Fermi level.

Table S1. Comparison with other reports on the CO_2RR to produce syngas.

Catalyst	Electrolyte	Current density ($mA\ cm^{-2}$) (CO/H_2)	Tuneable ratio CO/H_2	Stability (h)	Ref.
AgP_2 nanocrystals	0.5 M $KHCO_3$	0.28 (1:3) 2.46 (1:1)	1:3-5:1	12	(1)
Ag doped Co_3O_4	0.1 M $KHCO_3$	~ 7 (1:3)	1:4-5:4	10	(2)
silver nanowires	0.5 M $KHCO_3$	4 (1:1) 22 (3:2)	1:1-4:1	12	(3)
Ru (II) polypyridyl	0.5 M $NaHCO_3$	2.5 (1:4)	1:4-2:1	2	(4)
MoSeS alloy	4 mol% $EmimBF_4$ 96 mol% H_2O	-	1:1	10	(5)
$Zn_xCd_{1-x}S$-Amine	0.5 M $NaHCO_3$	~ 6 (1:1)	0-19.7	10	(6)
Co and Ni Single-Atom	0.5 M $KHCO_3$	> 74	0.23-2.26	7	(7)
Pd/C	0.5 M $NaHCO_3$	0.3 (3:4)	1:4-3:4	-	(8)
γ-In_2Se_3	30 wt% $[Bmim]PF_6$ 65 wt% MeCN 5 wt% H_2O	90.1 (1:1)	1:3-24:1	25	(9)
SnO_2/CuS	0.1 M $KHCO_3$	~5 (1:1) ~3 (1:3)	0.11-3.86	24	(10)
Zn-Ni	0.1 M KCl	8.4 (11:9)	-	50	(11)
Au/TiNS	0.5 M $KHCO_3$	-	0.3-3	-	(12)
PdH/TMN	0.5 M $NaHCO_3$	0.4 (3:4)	0.16-0.74	-	(13)
CdS_xSe_{1-x} nanorods	0.1 M $KHCO_3$	27.1	1:4-4:1	10	(14)
Co_3O_4-Cdots C_3N_4	0.5 M $KHCO_3$	0.25 (1:1)	0.07:1-4:1	30	(15)

MoS_2	EMIM-BF_4 solution (94 mol% water)	61 (4:1)	1:2-4:1	10	(16)
Zn	0.1 M $KHCO_3$	11.36 (7:6)	1:5-2.31:1	9.5	(17)
Fe-N-C	0.5 M $NaHCO_3$	-	0-4:1	10	(18)
Cu-enriched Au	0.5 M $KHCO_3$	30 (1:1)	-	8	(19)
Cu−In alloys	0.1 M $KHCO_3$	-	1:18-1:2.6	16.7	(20)
Cu	0.1 M $KHCO_3$	~7 (1:1)	9:16-32:1	-	(21)
carbon-supported Cu/In_2O_3	0.5 M $KHCO_3$	4.6 (1:4) 12.7(1:0.4)	1:4-1:0.4	5	(22)
R-Cu_3P/Cu	0.5 M $NaHCO_3$	36.3 (1:1) 82.9 (1:2) 115.0 (2:5) 130.0 (1:3)	0.1-2.24	> 20	This work

Table S2. Bader charge for the surface atoms of Cu_3P.

Atom	P	P	Cu	Cu	Cu	Cu	Cu	Cu
Charge	-0.56	-0.56	0.19	0.17	0.17	019	0.20	0.20

Table S3. Bader charge of CO_2 chemisorption on Cu_3P surface.

Atom	C	O	O	Tot
Charge	1.58	-1.08	-1.06	-0.56

References

(1) H. Li, P. Wen, D. S. Itanze, Z. D. Hood, X. Ma, M. Kim, S. Adhikari, C. Lu, C. Dun, M. Chi, Y. Qiu and S. M. Geyer, *Nat. Commun.,* 2019, **10**, 5724.

(2) S. -Y. Zhang, Y. -Y. Yang, Y. -Q. Zheng and H. -L. Zhu, *J. Solid State Chem.,* 2018, **263**, 44-51.

(3) W. Xi, R. Ma, H. Wang, Z. Gao, W. Zhang and Y. Zhao, *ACS Sustain. Chem. Eng.,* 2018, **6**, 7687-7694.

(4) P. Kang, Z. Chen, A. Nayak, S. Zhang and T. J. Meyer, *Energy Environ. Sci.,* 2014, **7**, 4007-4012.

(5) J. Xu, X. Li, W. Liu, Y. Sun, Z. Ju, T. Yao, C. Wang, H. Ju, J. Zhu, S. Wie and Y. Xie, *Angew. Chem. Int. Ed.,* 2017, **56**, 9121-9125.

(6) N. Meng, C. Liu, Y. Liu, Y. Yu and B. Zhang, *Angew. Chem. Int. Ed.,* 2019, **58**, 18908-18912.

(7) Q. He, D. Liu, J. H. Lee, Y. Liu, Z. Xie, S. Hwang, S. Kattel, L. Song and J. G.

Chen, *Angew. Chem. Int. Ed.,* 2020, **59**, 3033-3037.

(8) W. Sheng, S. Kattel, S. Yao, B. Yan, Z. Liang, C. J. Hawxhurst, Q. Wu and J. G. Chen, *Energy Environ. Sci.,* 2017, **10**, 1180-1185.

(9) D. Yang, Q. Zhu, X. Sun, C. Chen, W. Guo, G. Yang and B. Han, *Angew. Chem. Int. Ed.,* 2020, **59**, 2354-2359.

(10) X. Wang, J. Lv, J. Zhang, X. L. Wang, C. Xue, G. Bian, D. Li, Y. Wang and T. Wu, *Nanoscale,* 2020, **12**, 772-784.

(11) M. Beheshti, S. Kakooei, M. C. Ismail and S. Shahrestani, *Electrochim. Acta,* 2020, **341**, 135976.

(12) F. Marques Mota, D. L. T. Nguyen, J. -E. Lee, H. Piao, J. -H. Choy, Y. J. Hwang and D. H. Kim, *ACS Catal.,* 2018, **8**, 4364-4374.

(13) Y. Liu, D. Tian, A. N. Biswas, Z. Xie, S. Hwang, J. H. Lee, H. Meng and J. G. Chen, *Angew. Chem. Int. Ed.,* 2020, **59**, 11345-11348.

(14) R. He, A. Zhang, Y. Ding, T. Kong, Q. Xiao, H. Li, Y. Liu and J. Zeng, *Adv. Mater.,* 2018, **30**, 1705872.

(15) S. Guo, S. Zhao, X. Wu, H. Li, Y. Zhou, C. Zhu, N. Yang, X. Jiang, J. Gao, L. Bai, Y. Liu, Y. Lifshitz, S. -T. Lee and Z. Kang, *Nat. Commun.,* 2017, **8**, 1828.

(16) K. Lv, C. Teng, M. Shi, Y. Yuan, Y. Zhu, J. Wang, Z. Kong, X. Lu and Y. Zhu, *Adv. Funct. Mater.,* 2018, **28**, 1802339.

(17) B. Qin, Y. Li, H. Fu, H. Wang, S. Chen, Z. Liu and F. Peng, *ACS Appl. Mater. Inter.,* 2018, **10**, 20530-20539.

(18) T. N. Huan, N. Ranjbar, G. Rousse, M. Sougrati, A. Zitolo, V. Mougel, F. Jaouen

and M. Fontecave, *ACS Catal.,* 2017, **7**, 1520-1525.

(19) M. B. Ross, C. T. Dinh, Y. Li, D. Kim, P. De Luna, E. H. Sargent and P. Yang, *J. Am. Chem. Soc.,* 2017, **139**, 9359-9363.

(20) Z. B. Hoffman, T. S. Gray, K. B. Moraveck, T. B. Gunnoe and G. Zangari, *ACS Catal.,* 2017, **7**, 5381-5390.

(21) B. Kumar, J. P. Brian, V. Atla, S. Kumari, K. A. Bertram, R. T. White and J. M. Spurgeon, *ACS Catal.,* 2016, **6**, 4739-4745.

(22) H. Xie, S. Chen, F. Ma, J. Liang, Z. Miao, T. Wang, H. -L. Wang, Y. Huang and Q. Li, *ACS Appl. Mater. Inter.,* 2018, **10**, 36996-37004.